

Colossal Magnetoresistance of Ferromagnetic Manganites: Structural Tuning and Mechanisms

J. Fontcuberta, B. Martínez, A. Seffar, S. Piñol, J.L. García-Muñoz, and X. Obradors
*Institut de Ciència de Materials de Barcelona, Consejo Superior de Investigaciones Científicas,
 Campus Universitat Autònoma de Barcelona, Bellaterra 08193, Catalunya, Spain*
 (Received 19 June 1995; revised manuscript received 18 September 1995)

The amplitude $\Delta\rho(T,H)/\rho$ and temperature T_M , where the colossal magnetoresistance (CMR) response of $L_{1-x}Ca_xMnO_3$ manganites are maximum, are found to be controlled by the radius of the lanthanide (L^{3+}) which modifies the bending of the Mn-O-Mn bond. Increasing the bond distortion lowers T_M and enhances $\Delta\rho(T,H)/\rho$. Enhanced CMR arises from (1) a shift to lower temperatures of T_M , (2) a reduced mobility of the doping holes, and (3) an increase of the coupling between itinerant and localized electrons. The resistivity $\rho(H)$ follows an $\approx BM^2(H)$ law and the parameter B is also tuned by the Mn-O-Mn bond angle. The narrowing of the electronic bandwidth is the fundamental parameter controlling the observed CMR.

PACS numbers: 71.27.+a, 72.15.Gd, 72.20.My

Since the discovery of high- T_c superconductivity in copper oxides, transition-metal oxides of perovskite structure are receiving much attention. Of especial relevance are the effects of the strong correlation among free carriers and their interaction with the underlying antiferromagnetic background. One of the most exciting manifestations of this interplay is the recent observation of a colossal magnetoresistive (CMR) response of some La-A-Mn-O perovskite thin films [1–4].

Within the double-exchange interaction model [5] the itinerant charge carriers (holes) in the substituted $La_{1-x}A_xMnO_3$ (A is a divalent cation) oxide provide the mechanism for ferromagnetic interaction between $Mn^{3+/4+}$ ions. The ferromagnetic Curie temperature is related to the strength of the transfer integral t_{ij} between $Mn^{3+/4+}$ ions which itself controls the electronic (hole) conductivity. It follows that in this system one should expect a strong interplay between magnetic, transport, and structural properties.

However, detailed microscopic understanding of the magnetic properties and the structure of the doped phases is still lacking. A few possible mechanisms have been proposed for the CMR observed in the manganites. Some of them rely on the strong Hund coupling (J) between the moving carriers and the localized spins. Furukawa has recently developed a Kondo lattice model allowing evaluation of the spin disorder scattering [6] in terms of J/W where W is the electronic bandwidth. The particular case of infinite J has also been considered by Inoue and Maekawa [7] within the framework of a Hubbard-Kondo lattice model in the single band (U infinity) limit. The possible formation of spin polarons controlling the electrical conductivity [8] has also been examined. In spite of the intensive research effort, the interplay between crystallographic structure and the electrical and magnetic properties has remained hidden and the understanding and control on the giant magnetoresistance in these systems is still challenging.

The Zener-de Gennes mechanism for double exchange [5] offers a clear indication of a convenient way to control the coupling between the mobile holes and the localized t_{2g}^3 electrons. This coupling should be controlled by the transfer integral t_{ij} between Mn^{3+} -O- Mn^{4+} ions; then it can be expected that this coupling is strongly dependent on the angle subtended by the Mn-O-Mn bond. We will show in the following the success of such an approach. A consistent picture emerges and reveals that the structurally tuned electronic bandwidth (W) is the critical parameter governing the CMR. First, we will demonstrate that the ferromagnetic Curie temperature (T_M) is reduced by bending the Mn-O-Mn bond; the carrier mobility decreases when lowering the temperature ($T \geq T_M$), and the giant resistive peak occurring at T_M is enhanced as T_M lowers. As expected, carrier mobility becomes smaller as the band is narrowed. Second, we will demonstrate that the electrical resistivity (ρ) and the magnetization (M) can be approximately described by the relationship $\rho(T,H)/\rho(T,0) = 1 - B[M(T,H)/M_s]^2$, where M_s is the saturation magnetization. We will show that the parameter B increases when W is reduced. According to recently proposed models [6,7] the coefficient B is related to the coupling ($B \approx J/W$) between moving carriers and the localized spins. Agreement of the experimental data with theoretical predictions is striking. Our results provide, for the first time, a unique description of the colossal magnetoresistance of manganites and demonstrate that CMR can be tailored by appropriate structural engineering.

In this Letter we present data obtained on a series of $La_{1-y-x}L_xCa_yMnO_3$ oxides having a *fixed doping concentration* ($y = 0.3$); L is a rare-earth trivalent cation (Y, Dy, Yb, Gd). Substitutions ranging from $x = 0$ to 0.25 have been used, allowing us to explore variations of the mean ionic radii of the lanthanide ranging from 1.147 to 1.118 Å.

Ceramic samples of $La_{0.7-x}L_xCa_{0.3}MnO_3$ composition were prepared by solid state reaction of precursor oxides.

Appropriate amounts of La_2O_3 , CaO , Mn_2O_3 , and L_2O_3 ($L = \text{Y, Dy, Yb, and Gd}$) were mixed and heated in air at 900°C for 24 h with intermediate grinding. A final sintering process step was carried out at 1400°C in oxygen atmosphere. The as-prepared materials were characterized by x-ray and neutron diffraction and were found to be single phase with an orthorhombic ($Pbnm$) perovskite structure. The lattice parameters are found to vary linearly with the average ionic radius ($\langle r_A \rangle$) of the lanthanide. Magnetoresistivity measurements have been performed under fields up to 5.5 T by a conventional four-probe method with the current parallel to the applied field. Magnetic properties have been measured by using a quadrupole SQUID magnetometer up to 5.5 T.

Figure 1(a) shows the zero-field temperature dependence of the resistivity of some of the samples. Whereas at high temperature the resistivity is in the range of $0.1\text{--}0.3\ \Omega\text{ cm}$ and almost insensitive to the rare-earth substitution, a giant resistive peak develops at lower temperature (T_M). Its amplitude $\Delta R(T)/R = [R(T_M) - R(300\text{ K})]/R(300\text{ K})$ is of about $\approx 3 \times 10^5\%$ for $L = \text{Y}_{0.20}$. At temperatures well below

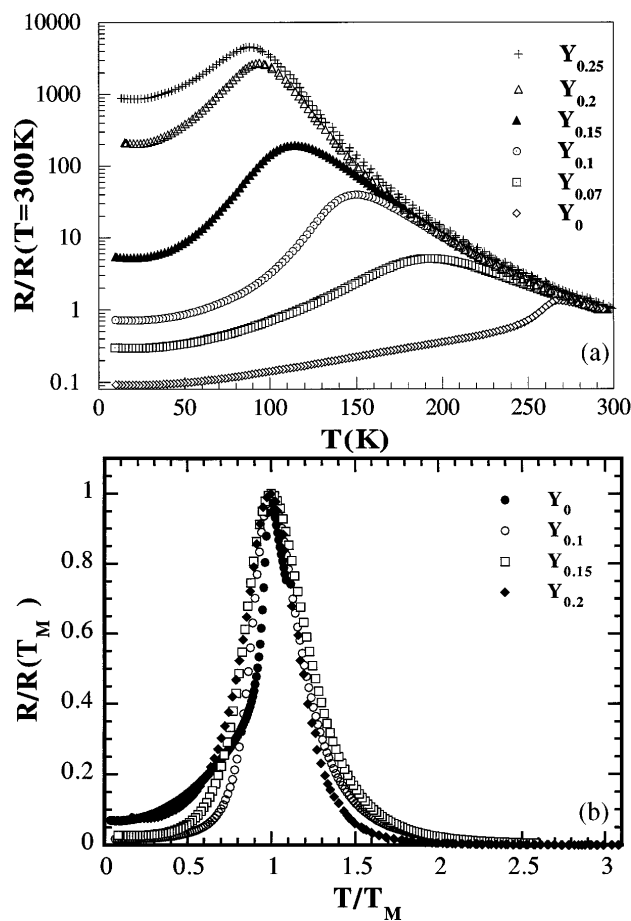


FIG. 1. (a) Normalized $[R(T)/R(300\text{ K})]$ resistivity vs temperature for $\text{La}_{0.7-x}\text{L}_x\text{Ca}_{0.3}\text{MnO}_3$ ($L = \text{Y}$, $x = 0, 0.07, 0.10, 0.15, 0.20$, and 0.25). (b) Dependence of the reduced resistivity $R(T)/R(T_M)$ vs the reduced temperature (T/T_M) for a selected set of samples.

the resistivity peak, a metalliclike behavior is almost recovered. The most remarkable result of Fig. 1(a) is the monotonous lowering of the temperature T_M where the maximum resistance occurs when reducing the mean size of the lanthanide ($\langle r_A \rangle$). This fundamental result is summarized in Fig. 2(a). The application of a magnetic field strongly reduces the resistivity. The magnetoresistance defined as $\Delta R(H)/R = [R(T_M, 0) - R(T_M, 50\text{ kOe})]/R(10\text{ K}, 50\text{ kOe})$ is temperature dependent and reaches its maximum at temperatures close to T_M , decreasing at temperatures above and below T_M .

As shown in Fig. 2(b), the amplitudes of the zero-field resistivity peak and the maximal magnetoresistance are closely related; both are controlled by the mean-ionic radii $\langle r_A \rangle$, increasing when decreasing $\langle r_A \rangle$ and T_M . It is important to emphasize that the value of $\langle r_A \rangle$ is the key parameter, irrespective of the rare-earth element.

We now focus our attention on the temperature dependence of the zero-field resistivity. We have found

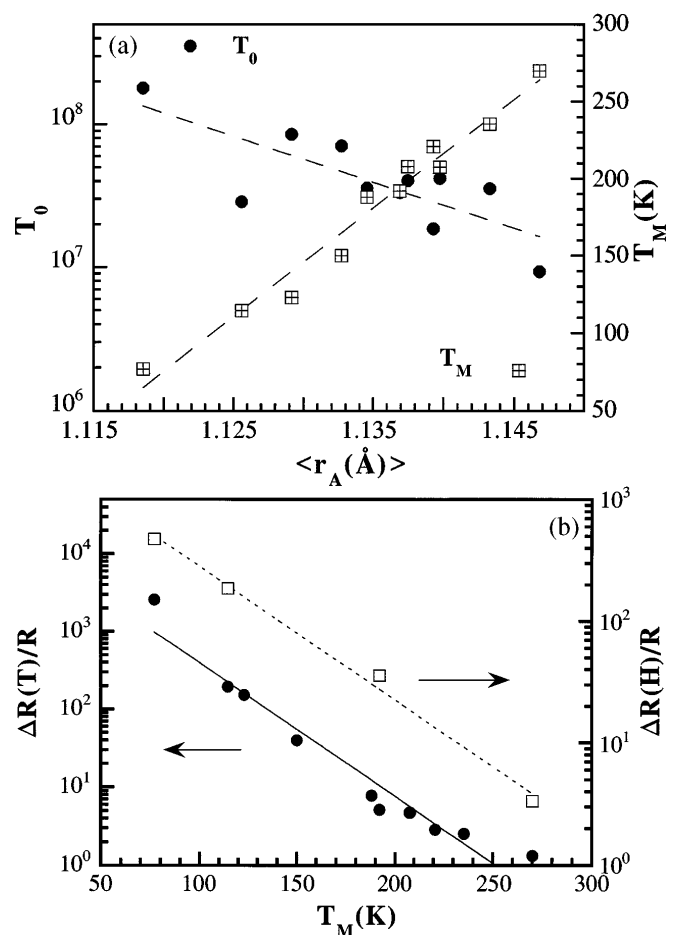


FIG. 2. (a) The zero-field temperature of the resistivity maximum (T_M) and T_0 (see definition in text) as a function of the averaged lanthanide radii. Dashed lines are only a guide to the eye. (b) Relative variations of the zero-field resistivity $\Delta R(T)/R = [R(T_M) - R(300\text{ K})]/R(300\text{ K})$ and magnetoresistance $\Delta R(H)/R = [R(T_M, 0) - R(T_M, 50\text{ kOe})]/R(10\text{ K}, 50\text{ kOe})$ vs T_M for several samples.

that at $T > T_M$ the functional dependence of $\rho(T, 0)$ is identical for all samples and consequently all resistivity curves are very similar when using $\rho(T, 0)/\rho(T_M, 0)$ and T/T_M as reduced variables; see Fig. 1(b). This observation reveals the existence of a common mechanism leading to the colossal rising of resistivity [9]. Even more, the amplitude of the maximum depends on the temperature T_M and on another parameter, $\rho(T_M, 0)$, which is characteristic of the sample. At temperatures above T_M and up to room temperature, $\rho(T)$ can be described by $\rho(T) = \rho_\infty \exp(T_0/T)^{1/4}$, with T_0 increasing monotonously with decreasing $\langle r_A \rangle$ [Fig. 2(a)]. Therefore, the colossal enhancement of $\Delta R(T)/R$ for samples of small $\langle r_A \rangle$ results from the occurrence of T_M at lower temperatures and from an enhanced T_0 value. The observed temperature dependence of the resistivity is believed to be related to the reduced carrier mobility when approaching the ferromagnetic ordering temperature. Although at present a detailed description of this process is not yet available, it is clear that rising of the T_0 values when increasing the bending of the Mn-O-Mn bond should reflect the enhancement of the carrier effective mass or the narrowing of the bandwidth. We recall here that the $\rho(T) = \rho_\infty \exp(T_0/T)^{1/4}$ law is typically found when conduction takes place by hopping between localized states. Within this model the T_0 parameter is related to the spatial extension (l) of the localized states and to the density of states [$g(E_F)$]: $l \approx [g(E_F)T_0]^{-1/3}$. It may also be expected that bending of the Mn-O-Mn bond could result in an enhancement of $g(E_F)$. The observation that when reducing $\langle r_A \rangle$ the measured T_0 increases indicates that the reduction of l is the main factor determining the T_0 enhancement. Therefore, our data suggest that the decrease of the bandwidth associated to an increase of the lattice distortion decreases the localization length and thus the carrier mobility is reduced. Detailed measurements of $g(E_F)$ are not yet available but a very rough estimate can be obtained if one assumes a free charge density of $\approx 10^{21} \text{ cm}^{-3}$ and a parabolic band. Under these assumptions $l \approx 1 \text{ \AA}$. Although this value is somewhat smaller than expected, probably due to the fact that the parabolic band approximation is too rough and to the fact that only a small fraction of the doping carriers appears to be involved in the conduction process [1,5], it is of the right order of magnitude and provides support to the variable range hopping analysis.

In terms of the perovskite tolerance factor $t = (r_A + r_0)/(r_B + r_0)\sqrt{2}$, the cubic perovskites have $t \approx 1$ where r_A , r_0 , and r_B represent the ionic radii of the lanthanides, oxygen, and transition-metal ions, respectively. The B-O-B bonds close when reducing t and lower the lattice symmetry. Consequently, in the present orthorhombic samples, substitution of La^{3+} by smaller lanthanides L^{3+} results in an enhanced distortion of the cubic perovskite. Figure 2(a) shows us that T_M is shifted towards lower temperatures when the tolerance factor is reduced.

In addition, our neutron diffraction data reveal that the cell symmetry remains intact and the mean Mn-O-Mn bond angle (Φ) closes when reducing $\langle r_A \rangle$. For instance, we have found that $\Phi = 158.3(5)^\circ$ for $L = \text{Y}_{0.15}$ and $\Phi = 159.7(5)^\circ$ for $L = \text{Y}_{0.05}$ [10]. This situation is analogous to that encountered in the LNiO_3 perovskites ($L = \text{Pr, Nd, Sm, \dots}$) where it has been shown that the main effect of changing the lanthanide is to modify the Ni-O-Ni bond angle without significant variations of the Ni-O distances in the NiO_6 octahedra [11]. The consequences of these subtle variations of the Ni-O-Ni bond angle on the electronic properties are extraordinary because modifications of the bandwidth (through t_{ij}) trigger the metal-insulator transition [12].

Our results reveal that structural distortion is the key parameter controlling the CMR response: Increasing the distortion enhances $\Delta R(T, H)/R$ and decreases T_M . We have shown that two main reasons lead to the higher magnetoresistance of samples having smaller $\langle r_A \rangle$: (a) the pronounced increase of resistivity at $T \approx T_M$ when T_M is lowered and (b) their reduced carrier mobility (i.e., higher T_0 values). Both factors appear to be controlled by the electronic bandwidth, which itself is tuned by the bending of the Mn-O-Mn bond.

In Fig. 3 we plot the field dependence of the resistivity of several samples at various temperatures as a function of the magnetization. In order to allow comparison of measurements performed at distinct temperatures, the reduced variables ρ/ρ_0 and M/M_s are used where M_s is the saturation magnetization and $\rho_0 \equiv (T, 0)$ is the zero-field resistivity. Each set of data in Fig. 3 contains isothermal $\rho(T, H)$ and $M(T, H)$ measurements on a given sample ($L = \text{Y}$; $x = 0, 0.07, \text{ and } 0.15$) performed at temperatures close to the corresponding maximum T_M . For clarity only a few representative temperatures are shown. The first observation in Fig. 3 is that all data for each sample collapse onto a single curve, thus showing that a unique relationship exists between the magnetoresistance and the

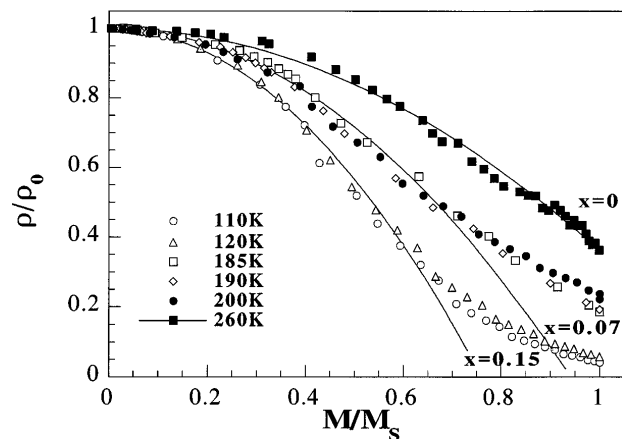


FIG. 3. Reduced resistivity $\rho(T, H)/\rho_0$ vs reduced magnetization $M(T, H)/M_s(T, 5 \text{ T})$ data for samples $L = \text{Y}$, $x = 0, 0.07, \text{ and } 0.15$ at several temperatures. The lines through the data are the fits by the $B(M/M_s)^2$ expression.

magnetization. The lines through the data are the fits to the $\rho(T, H)/\rho_0 = 1 - B[M(T, H)/M_s]^2$ expression. For the $x = 0.15$ sample, i.e., the sample having the lowest T_M and maximal magnetoresistance in Fig. 3, the fitted B parameter is $B \approx 1.7$, whereas for the $x = 0.07$ and 0 samples B decreases to 1.14 and 0.66, respectively. It is clear that the B parameter reflects an intrinsic characteristic of the sample. It can also be appreciated in Fig. 3 that in the high magnetization region the quadratic dependence fails and the resistivity has a weaker $\rho(M)$ dependence.

Within the framework of some recently proposed theoretical models [6,7], the parameter B is related to the coupling ($B \approx J/W$) between moving carriers and the localized spins: Larger B corresponds to stronger coupling. Accordingly, our data indicate that this coupling reinforces as the Mn-O-Mn bond bends. That is, J/W increases as the bandwidth (W) becomes narrower. This observation stresses the fundamental role played by the bandwidth, and thus the density of states, on the CMR and supports the conclusions presented above which were extracted from zero-field data.

It may be useful to compare the values of B to the theoretical estimates. In the limiting case of $J \rightarrow \infty$, Inoue and Maekawa [7] predicted $B = 7/4$, whereas Furukawa [6] found B to increase continuously from $B = 1$ for $J/W \approx 1$ to $B \approx 4-5$ at higher coupling $J/W \approx 5$. Our results for $x = 0.15$ nicely agree with the predictions of Inoue and Maekawa and fall within the predicted range from the Furukawa model. However, it is not clear at this moment to what extent this agreement is significant because theoretical predictions were obtained for systems with fixed density of states. It should also be noted that the progressive departure of the quadratic $\rho(M)$ dependence (Fig. 3), when increasing the magnetization, has also been predicted for systems of enhanced coupling [6]. Accordingly, for samples $x = 0$ and 0.07 the quadratic $\rho(M)$ law extends to higher magnetization values than for sample $x = 0.15$.

Recently, the Kondo lattice model has been extended [13] to account for the dependence of T_M on the coupling J parameter, assuming a fixed density of states. It was found that, as physical intuition indicates, T_M increases with increasing J . On the other hand, the ordering temperature is expected to increase with the free carrier bandwidth because of the enhanced kinetic energy of carriers at the ferromagnetic state [5]. In the present case, the progressive bending of the Mn-O-Mn bond should reduce T_M . Our observation that enhanced coupling occurs simultaneously with a reduction of T_M appears to indicate that the reduction of the bandwidth dominates T_M and the coupling parameter B .

In conclusion, the present work clearly shows that the colossal magnetoresistance of the manganese perovskites results from the interplay between the itinerant charge carriers and the localized moments and this interaction can be conveniently controlled by appropriate structure engineering. One of our major findings is that, at a fixed charge

carrier density, the intensity of the CMR increases when lowering the onset of ferromagnetic order and this lowering of T_M is associated to a narrower bandwidth. Collapsing of the bandwidth results in a reduced mobility of the carriers before the ferromagnetic order is established and thus in an even higher resistivity at T_M . This is the dominant factor on the CMR. Our results impose serious constraints for any further theoretical development and may have also important consequences for potential technological applications. We have also shown that the field dependence of the resistivity of these samples is well described by the $B(M/M_s)^2$ law. It has been found that the coupling (J/W) is reinforced by the reduced bandwidth accompanying the enhanced bond distortion. Finally, we have demonstrated that CMR can indeed be tailored in manganese perovskites and further achievements related to even higher colossal magnetoresistance can be expected.

We acknowledge financial support by the CICYT-MIDAS (MAT94-1924-CO2), DGICYT (PB92-0849) projects, and the Generalitat de Catalunya. A.S. is grateful to the Instituto de Cooperación con el Mundo Árabe for a grant.

Note added.—During the process of revision of this Letter correlations between magnetization M and electrical resistivity ρ in the region beyond saturation were reported by Hundley *et al.* [14].

-
- [1] R. von Helmolt, J. Wecker, B. Holzapfel, L. Schultz, and K. Samwer, Phys. Rev. Lett. **71**, 2331 (1993).
 - [2] S. Jin, T.H. Tiefel, M. McCormack, R.A. Fastnacht, R. Ramesh, and L.H. Chen, Science **264**, 413 (1994); S. Jin, H.M. O'Bryan, T.H. Tiefel, M. McCormack, and W.W. Rhodes, Appl. Phys. Lett. **66**, 382 (1995).
 - [3] G.H. Jonker and J.H. Van Santem, Physica (Utrecht) **19**, 120 (1953).
 - [4] E.O. Wollan and W.C. Koehler, Phys. Rev. **100**, 545 (1955).
 - [5] C. Zener, Phys. Rev. **81**, 440 (1951); P. de Gennes, Phys. Rev. **118**, 141 (1960).
 - [6] N. Furukawa, J. Phys. Soc. Jpn. **63**, 3214 (1994).
 - [7] J. Inoue and S. Maekawa, Phys. Rev. Lett. **74**, 3407 (1995).
 - [8] T. Kasuya and A. Yanase, Rev. Mod. Phys. **40**, 684 (1968).
 - [9] J. Fontcuberta *et al.* (to be published).
 - [10] J.L. García-Muñoz *et al.* (to be published); after submission of the paper H.Y. Hwang *et al.* [Phys. Rev. Lett. **75**, 914 (1995)] have also confirmed the same angular dependence.
 - [11] J.L. García-Muñoz, J. Rodríguez-Carvajal, P. Lacorre, and J.P. Torrance, Phys. Rev. B **46**, 4414 (1992).
 - [12] J.B. Torrance and R. Metzger, Phys. Rev. Lett. **63**, 1515 (1989); X. Obradors, L.M. Paulius, M.B. Maple, J.B. Torrance, A.I. Nazzari, J. Fontcuberta, and X. Granados, Phys. Rev. B **47**, 12353 (1993).
 - [13] N. Furukawa (to be published).
 - [14] M.F. Hundley *et al.*, Appl. Phys. Lett. **67**, 860 (1995).